APPENDIX A

Magnetic Theory and Background

When conducting magnetic analyses it is imperative to determine the magnetic mineralogy, grain-size, and concentration of the various magnetic components within a sample. Therefore, multi-parametric magnetic techniques are needed to identify and quantify the magnetic properties of a sample. This section discusses magnetic theories and techniques utilized in this study to characterize samples based on their magnetic properties.

Magnetic Susceptibility

Magnetic susceptibility is a measure of the degree to which a substance affects a known magnetic field and is a function of the concentration, grain-size, and type of magnetic minerals present in a sample (Begét et al., 1990). Two types of magnetic susceptibility measurements are commonly used to infer specific magnetic grain-sizes and concentrations.

Volume Magnetic Susceptibility (κ)

Using a Bartington MS2 susceptibility meter with surface scanning sensor (MS2K), volume magnetic susceptibility (κ) can be measured in the field or in the laboratory. κ is a bulk measurement that groups all of the magnetic subpopulations present in a sample into one bulk value, $\kappa = M/H$, where M is the magnetization created in the sample and H is the field applied; both are in units of Am^{-1} and therefore κ is dimensionless (expressed as SI units). Since measurements of κ do not account for mass, the measurements are sensitive to changes in the bulk density of the material being measured.

Frequency-dependent magnetic susceptibility (χ_{fd})

χ_{fd} is measured on a mass per unit volume basis. The Bartington Instruments MS2B Dual Frequency Sensor measures χ within an AC magnetic field amplitude of 80 Am^{-1} at low frequency (465 Hz) and high frequency (4650 Hz). Samples are measured at each frequency to obtain values corresponding to the low (κ_{lf}) and high (κ_{hf}) frequencies. Measurements made at these two frequencies are corrected for mass to account for any bulk density differences between the samples. This allows for an accurate and easier comparison of κ, since κ is sensitive to changes in bulk density. Mass dependent susceptibility (χ) is determined by:

$$\chi = \kappa/\rho \ [m^3 \ kg^{-1}] \qquad \textbf{eq. 1}$$

where ρ is bulk density and is equal to sample mass (kg)/ sample volume (m^3). Samples were measured at each frequency such that low-frequency mass-dependent susceptibility (χ_{lf}) = κ_{lf}/ρ [m^3 kg^{-1}] and high-field mass-dependent susceptibility (χ_{hf}) = κ_{hf}/ρ [m^3 kg^{-1}]. Frequency-dependent susceptibility can be expressed as a percentage loss of susceptibility,

$$\chi_{fd\%} = \{(\chi_{lf} - \chi_{hf})/\chi_{lf}\} \ x \ 100 \qquad \textbf{eq. 2}$$

Measurements made at these two frequencies are generally used to detect the presence of ultrafine (< 0.03 μm) superparamagnetic (SP) minerals occurring as crystals produced by bacteria or by mineral authigenic chemical processes occurring in soils. Samples where SP minerals are present will show slightly lower values when measured at high frequency; samples without the superparamagnetic minerals will show identical κ values at both frequencies (Dearing, 1999). Table 1 outlines the suggested $\chi_{fd\%}$ values for the occurrence SP grains in a environmental samples.

Table 1 Interpretation of $\chi_{fd\%}$ values. When $\chi_{fd\%}$ > 10% use $\chi_{fd\%}$ as an estimate of SP concentration. (From Dearing, 1999).

Low $\chi_{fd\%}$	< 2.0	Virtually no SP grains
Medium $\chi_{fd\%}$	2.0-10.0	Mixture of SP and coarser grains, or SP grains < 0.05 μm
High $\chi_{fd\%}$	10.0-14.0	Virtually all SP grains
Very high $\chi_{fd\%}$	>14.0	Erroneous measurement, anisotropy, weak sample or contamination

Hysteresis Parameters

Hysteresis measurements conducted at the UC Davis Paleomagnetism were used to identify specific magnetic mineralogies, grain-sizes, and concentrations within the samples. Hysteresis parameters were obtained by cycling a sample between a very strong magnetic field applied in one direction and an equal but opposite magnetic field in the other direction. By doing this, a sample responds (on the basis of its magnetic minerals, grain size, concentration, and grain shape) to these applied field cycles (field strength is measured in Tesla (T)) by creating its own magnetism, or magnetization (magnetization measured in Am^2). Four parameters (see Fig. A-1) can be derived from hysteresis data; the saturation magnetization (M_S, in Am^2), saturation remanent magnetization (M_R, in Am^2), coercivity (B_C, in T), and the coercivity of remanence (B_{CR}, in T). These parameters, and the ratios derived from them provide additional methods for determining magnetic mineralogy, magnetic grain size, and magnetic concentration, as described below.

M_S is equivalent to the amount of magnetization produced at saturation (saturation is the point where the material cannot acquire any more magnetism with increased field). M_S is lower for ferrimagnetic minerals because they are the easiest to magnetize. In cases where the sample is dominated by weaker magnetic minerals (antiferromagnetic, paramagnetic, and diamagnetic), extreme fields (up to 3 T) are needed to saturate the sample. Standard laboratory instruments cannot achieve these high fields, therefore the true saturation magnetization cannot be determined for these minerals. However, the magnetization created in the sample from the maximum field applied is considered to be the saturation magnetization. Removal of this saturating field leaves the sample with its M_R. M_R is the amount of magnetism remaining in a sample after exposure to a forward saturating field, or the maximum field attainable. Application of a reverse field leads to a point where the overall magnetization is zero (where $M = 0$ on hysteresis loop, Fig. A-1). The field necessary to achieve this is B_C (Fig. A-1). To arrive back at the origin (point where the sample has zero remanent magnetism), a somewhat stronger reverse field is necessary; this field is B_{CR} (Fig. A-1). Slope corrected hysteresis loops (described below) allow M_S, M_R, B_C, and B_{CR} to be discriminated on the basis of individual magnetic mineral types (para-, dia-, antiferro-, ferrimagnetic, or ferromagnetic).

Magnetic Mineral Types

Five major groups of magnetic materials are recognized:

1. Diamagnetism
2. Paramagnetism
3. Antiferromagnetism
4. Ferrimagnetism
5. Ferromagnetism

Diamagnetism is very weak and arises in materials where all the orbital shells are filled and there are no unpaired electrons. Due to the interactions of an applied magnetic field and the motion of electrons orbiting the nucleus, diamagnetic materials have no net magnetic moments (Tarling and Hrouda, 1993). Electrons spin about their own axis while orbiting the nucleus of an atom. Each creates its own magnetic moment, one from electrons spinning about their own axis, and the other from the orbital spin of electrons about the nucleus. This gives rise to a spin magnetic moment and an orbital magnetic moment. The vector sum of these two moments is aligned in the opposite direction to the applied field. In diamagnetic minerals, this is due to Lorentz forces (the sideways motion of electrons around a nucleus in the presence of an applied field) that result in Larmor precession of electron orbits (generated by orbital torque from the Lorentz forces) (Evans and Heller, 2003). Magnetism that arises from diamagnetic materials is therefore negative in the presence of a forward field. For this reason, κ and χ are negative for diamagnetic substances (e.g. water, quartz, feldspar, calcite, kaolinite). Upon removal of the applied field, the vector sum of the two magnetic moments is zero. This is due to opposing spin states of each magnetic moment where the orbital spin moments perfectly counter the electron spins and as a result cancel each other out, leaving a total magnetic moment of zero. Hysteresis loops also show this effect (Fig. A-2): at high forward fields ($+B$) the magnetization (M) acquired by the sample is negative and decreases to zero as the field (B) is removed. Application of a reverse field ($-B$) then causes the magnetization to increase in the positive direction. The loop follows the same path when the negative applied field ($-B$) is reversed.

Paramagnetism arises due to the interactions of unpaired electrons in partially filled orbitals. Due to these interactions, paramagnetic materials (e.g. siderite, biotite, and pyrite) have a net magnetic moment due to the partial alignment of magnetic moments in the direction of the applied field (Tarling and Hrouda, 1993). As in diamagnetism, removal of the external field causes the magnetization to return to zero due to electron spin moments and orbital moments canceling each other out. These relationships are illustrated in Figure A-3. As the magnetic field ($+B$) is decreased to zero, the magnetization ($+M$) decreases to zero and no magnetic moment remains. Application of a reverse field ($-B$) results in a negative magnetization ($-M$) that increases towards negative saturation. The loop follows the same path when the negative applied field ($-B$) is reversed.

Ferrimagnetic and antiferromagnetic behavior arises from the alignment of spin magnetic moments of electrons in the incompletely filled 3*d* subshell (Thompson and Oldfield, 1986). Iron, for example is 4 electrons short of having a filled 3*d* subshell. Following Hund's rule, this 3*d* shell has five electron spins aligned in the same direction and one electron spin opposing, so there is a net magnetic moment in one direction (Evans and Heller, 2003). Unlike paramagnetism and diamagnetism, ferrimagnetic materials (e.g. magnetite, greigite, and pyrrhotite) have anti-parallel spin alignments that result from super-exchange forces (where the exchange coupling force extends over an intermediate anion). This causes the electron spins in adjacent cations to be reversed, creating two oppositely magnetized, but intimately mixed lattices within the material (Tarling and Hrouda, 1993). Since ferrimagnetic and antiferromagnetic materials have an uneven number of electrons, they can acquire a permanent magnetization, or remanence, after exposure to a magnetic field. Remanence is responsible for M_R (Fig. A-1) not falling in the origin, as it does for diamagnetic and paramagnetic materials (Figs. A-2 and A-3, respectively). More simply, when an applied field is removed ($B = 0$; Fig. A-1), ferrimagnetic and antiferrimagnetic minerals are still magnetized ($M > 0$). Hysteresis loops of ferrimagnetic and antiferromagnetic samples are shown in Figures A-4 and A-5, respectively. Due to lower coercivities (B_{CR} ferrimagnetic < B_{CR} antiferromagnetic), ferrimagnetic materials have hysteresis loops that are narrower about the origin than antiferromagnetic loops (Figs. A-4 and A-5). This is due to the fact that ferrimagnetic materials are easier to demagnetize than antiferromagnetic materials, such as hematite and goethite.

Ferromagnetic materials, such as iron, cobalt, and nickel have atomic moments that exhibit very strong interactions (due to exchange forces) and result in parallel alignment of atomic moments. This parallel alignment produces a large net magnetization, even in the absence of an applied field, giving rise to a spontaneous magnetization, which is the net magnetization that exists inside ferrimagnetic and ferromagnetic materials in the absence of an applied field (Thompson and Oldfield, 1986). Ferromagnetic materials have crystalline structures and are normally compounds of transition metals like iron, nickel, and cobalt (Smith, 1999). Ferrimagnetic materials, in contrast, have antiparallel atomic moments and are commonly iron oxides with a spinel structure (Thompson and Oldfield, 1986).

Magnetic Grain Size

Magnetic grain-size measurements were estimated using two hysteresis ratios, M_{RS}/M_S vs. B_{CR}/B_C, obtained by the above mentioned hysteresis parameters. Magnetic grain sizes play an important role in controlling the magnetic properties of natural samples (Dunlop, 2002). The five magnetic groups can be subdivided based on grain size into (from largest to smallest) multidomain (MD), pseudo-single domain (PSD), single domain (SD), and superparamagnetic (SP). These so-called ‘domains’ arise due to competition between magnetic forces within the material and are produced by the attempt to minimize the overall energy state of the magnetic grain (Dunlop and Ozdemir, 1997). Surface charges form at the ends of grains (See Fig. A-6) to create a second source of a magnetic field (the demagnetizing field) and the energy associated with this demagnetizing field is called the magnetostatic energy (Moskowitz, 1991). The magnetostatic energy can be reduced to approximately one-half if the magnetization splits into two domains magnetized in opposite directions, bringing (+) and (-) charges closer together, and thereby decreasing the extent of the demagnetizing field (Moskowitz, 1991). Domain walls (see Fig. A-6) separate these regions of opposing magnetization directions, and within these walls, the magnetization changes 180^o from one domain to the next (Dunlop and Ozdemir, 1997). The number of domains within a grain is a function of its size and shape (Dunlop and Ozdemir, 1997). Generally, larger grains can accommodate multiple domains (hence multidomain) whereas smaller grains can only accommodate one domain (hence single domain). Domain states in different magnetic minerals will have different associated grain sizes, but in general, the larger the grain size the more domains it contains.

Multidomain (MD) grains consist of mineral grains that contain many domains, whereas those that contain only one domain are termed single domain (SD). The boundary between the two distinctions is not sharp – there is a significant middle ground of grains that contain only a few domains (Evans and Heller, 2003). In the strictest sense, such grains are MD. However they possess many of the properties common to SD grains (Evans and Heller, 2003). These ‘middle ground’ grains are termed pseudo-single-domain (PSD) and possess a mixture of SD-like (high remanence) and MD-like (low coercivity) behavior (Moskowitz, 1991). Within the SD range, as particle size continues to decrease, a critical threshold is reached. At this point the remanence and coercivity go to zero and the grain becomes superparamagnetic (SP). The shape of hysteresis loops is partially determined by magnetic grain size. SD loops are typically wider than loops for MD materials; this is a refection of higher coercivity and remanence in SD material.

The Day Plot

Hysteresis properties are useful for indicating domain state, and indirectly, the grain size of magnetite. This is done by plotting a graph of M_{RS}/M_S vs. B_{CR}/B_C, as developed by Day et al. (1977) and further developed by Dunlop and Ozdemir (1997) and Dunlop (2000). This method discriminates between the different domain states of magnetite, and graphically depicts grain size as a function of domain state. The ratio M_{RS}/M_S is greatest for SD particles and decreases as particle size increases into the PSD and MD fields (Evans and Heller, 2003). Figure A-7 illustrates these relationships for magnetite.

Interpreting Hysteresis Loops and Parameters

Based on the hysteresis properties of diamagnetic, paramagnetic, ferrimagnetic, and antiferromagnetic materials, it possible to separate each of these magnetic characteristics from a mixture of magnetic assemblages. Kelso et al. (2002) outlines four methods of separation that have been documented in the literature: (1) a mathematical method based on site analysis; (2) measurement of anisotropy of remanence; (3) utilizing the temperature dependence of susceptibility; and (4) utilizing the field dependence of susceptibility. Methods 3 and 4 are used in this analysis and are based upon the different response of diamagnetic, paramagnetic, antiferromagnetic, and ferrimagnetic minerals to temperature and large applied fields (up to 1.2 T). Method 3 is discussed in more detail in the thermal analyses section below.

Method 4 is based upon the field response of susceptibility as a function of magnetic mineral type. With an increase in applied field (B), the magnetization (M) for diamagnetic and paramagnetic minerals behaves linearly but in opposite directions (Figs. A-2 and A-3; Kelso et al., 2002). In contrast, ferrimagnetic minerals tend to saturate (M_S) at lower applied fields, such that the magnetization (M) no longer increases with increased field (H) (Fig. A-4). Antiferromagnetic saturation is reached at fields well above those attainable by standard laboratory equipment. However, differences in coercivity and loop-shape commonly allow their distinction within common laboratory fields (~1 T). Separation of these magnetic mineral types and the field dependence of susceptibility are discussed below.

Mixtures of different mineral magnetic assemblages, be it assorted mineral types, granulometry, and/or concentration, give rise to distinct magnetic patterns that can be distinguished on the basis of hysteresis data. For rocks that have both ferrimagetic and paramagnetic minerals, changes in magnetization at fields above ferrimagnetic saturation are primarily due to either diamagnetic, paramagnetic or antiferromagnetic susceptibility (κ in Figs. A-2 and A-3), where κ is the slope of the loop at fields above ferrimagnetic saturation (~0.2 - 0.8 T). When corrected for mass, κ is symbolized as χ_h to give the high-field susceptibility. χ_h is equivalent to the paramagnetic + antiferromagnetic susceptibility (the paramagnetic and antiferromagnetic contribution to χ_{lf}). If no antiferromagnetic minerals occur in the sample, χ_h is simply the paramagnetic susceptibility. For diamagnetic loops, κ is the slope of the loop at fields above ferrimagnetic saturation (Fig. A-2). When the diamagnetic slope is corrected for mass, κ is symbolized as χ_d. The difference between χ_h or χ_d and χ_{lf} gives the ferrimagnetic susceptibility (χ_{ferri}) which is the ferrimagnetic contribution to χ_{lf}. When there is no evidence of antiferromagnetic contribution, correcting hysteresis data for slope also yields hysteresis parameters (M_R, M_S, B_C) for the ferrimagnetic fraction. By subtracting the ferrimagnetic parameter values from the total combined values of the sample, paramagnetic and/or diamagnetic parameters can be separated quantitatively. When antiferromagnetic minerals are present it is difficult to quantitatively separate the ferrimagnetic contribution from hysteresis parameters alone. This is due to the fact that moment measurements are effected by each mineral type and represent the collective contributions from each.

The hysteresis loop shown in Figure A-8 is an example of a mixture of quartz and hematite and illustrates the characteristic patterns of diamagnetic and antiferromagnetic minerals (see Figs. A-2 and A-5, respectively). In figure A-8, the loop is closed at higher fields and the slope is negative, whereas at lower fields the loop remains open and the slope is positive about the origin. The presence of an antiferromagnetic component is inferred because: 1) the slope deflects at lower fields, and 2) the loop is open at fields above 0.4 T. The hysteresis loop shown in Figure A-9 is an example of a mixture of quartz and magnetite, and illustrates the characteristic patterns of diamagnetic and ferrimagnetic minerals (see Figs. A-2 and A-4, respectively. As in Figure A-8, the loop in Figure A-9 is closed at higher fields and the slope is negative. However, since ferrimagnetic minerals have lower M_S and B_{CR} values compared to antiferromagnetic minerals, the loop is more constricted at lower fields and closes at fields below

~ 0.4 T. One important fact to point out is that diamagnetic mineral assemblages are easily masked by the presence of stronger antiferromagnetic or ferrimagnetic minerals. Therefore, in Figures A-8 and A-9, the concentration of antiferromagnetic and ferrimagnetic minerals, respectively, is small enough such that the diamagnetic components dominate and the overall slope of the loop is negative.

Mixtures of ferrimagnetic and paramagnetic grains produce hysteresis loops that are slope positive at low and high fields (Fig. A-10). The presence of ferrimagnetic minerals is inferred because the slope is deflected at low fields and is closed at fields < 0.6 T. Mixtures of antiferromagnetic and paramagnetic grains (Fig. A-11) produce hysteresis loops that are also slope positive at both low and high fields. The presence of antiferromagnetic components is inferred because the slope is deflected at low fields and because the loop closes at fields above 0.6 T.

The above examples represent simple mixtures of diamagnetic, paramagnetic, antiferromagnetic, and ferrimagnetic mineral types. Natural samples, however, are subject to different mixtures of mineral types, magnetic grain sizes, and magnetic concentrations. Mixed magnetic component hysteresis loops can be corrected for either χ_h or χ_d to yield loops composed solely of the ferrimagnetic component (e.g. slope correcting Fig. A-10 will yield Fig. A-4). Then M_S, M_R, and B_C can be determined for the ferrimagnetic fraction. Subtracting these parameters from the original (non-slope corrected) loop yields values for paramagnetic and antiferromagnetic components. Therefore, these other parameters need to be considered in order to properly explain the magnetic characteristics of natural samples.

Roberts et al. (1995) developed a method that discriminates the magnetic components within mixed mineral and grain size distributed magnetic systems. They postulate that "wasp-waisted" hysteresis loops (loops that are constricted in the middle, but wider above and below (Fig. A-12) are a relict of: (1) the coexistence of at least two magnetic components with strongly contrasting coercivities due to either mixtures of different grain sizes of a single magnetic mineral, or a combination of magnetic minerals with contrasting coercivities, or a combination of both situations; (2) materials with high $\mathrm{B}_{\mathrm{CR}}/\mathrm{B}_{\mathrm{R}}$ ratios; (3) low coercivity components comprising a large fraction of the total volume of magnetic grains (where $B_{CR}/B_R \geq 10$); (4) mixtures of superparamagnetic (SP) and single-domain (SD) grains, which are more likely to give rise to wasp-wasted loops than equivalent mixtures of SD and multi-domain (MD) grains; and (5) large concentrations of minerals with weak magnetic moments (i.e. hematite) mixed with ferrimagnetic minerals (i.e. magnetite).

Thermal Magnetic Analyses

Temperature-dependent susceptibility measurements (TDS) were conducted on a Kappabridge KLY-3S with CS-3 furnace apparatus from room-temperature to 700°C and then back. Sequential step-wise heating experiments were conducted on selected samples by measuring hysteresis properties at room-temperature after each heating step. Both experiments were conducted at the UC Davis Paleomagnetism Laboratory.

Thermal treatment of magnetic minerals often leads to the destruction and formation of new mineral phases. The thermal alteration of magnetic minerals can correspond to the appearance of a new ferrimagnetic mineral from paramagnetic phases, the transformation of ferrimagnetic phases into other ferrimagnetic minerals, or to grain-size and structural changes of ferrimagnetic carriers (Henry et al., 2005). The most widely used method for detecting these thermal alterations is temperature-dependent susceptibility. This method measures the variations of bulk magnetic susceptibility at room temperature after successive thermal steps. Acquisition of temperature-dependent susceptibility cooling and heating curves helps identify the magnetic minerals in a sample (Hrouda et al., 2003). Diamagnetic minerals exhibit no temperature variation of susceptibility. Paramagnetic minerals behave in accordance to the Curie-Weis Law: $\kappa = C/T$, where, C is a constant and proportional to the concentration of paramagnetic ions, and T is absolute temperature. Therefore, the paramagnetic susceptibility is inversely proportional to absolute temperature. Ferrimagnetic minerals carry a remanent magnetization below a critical temperature, called the Curie temperature. However, above this temperature thermal activation energies disrupt the ordering of magnetic moments and ferrimagnetism is lost resulting in paramagnetic behavior. Antiferromagnetic ordering is also destroyed by thermal agitations at the Curie temperature. Curie temperatures occur at a critical point that is specific for each mineral. The degree of purity and/or lattice substitutions within a mineral may affect the temperature at which the Curie temperature is reached resulting in slightly higher or lower Curie temperatures.

Temperature-dependent susceptibility (TDS) measurements are effective in identifying mineralogy. However, the measured values reflect only the result of all the simultaneous changes in a complex mineral system such as a natural rock (Henry et al., 2005). Another thermal method for detecting mineral alterations is hysteresis acquisition after the sequential step-wise heating of a sample. Recently, a study based on the comparison of hysteresis loops measured at room temperature after successive heating steps revealed that the processes of grain growth, oxidation, stress release, and phase transformations can be evaluated using this technique (Henry et al., 2005).

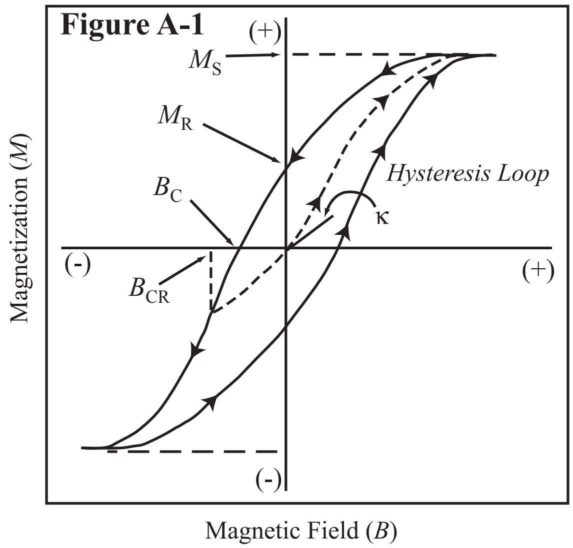
Figure A-1

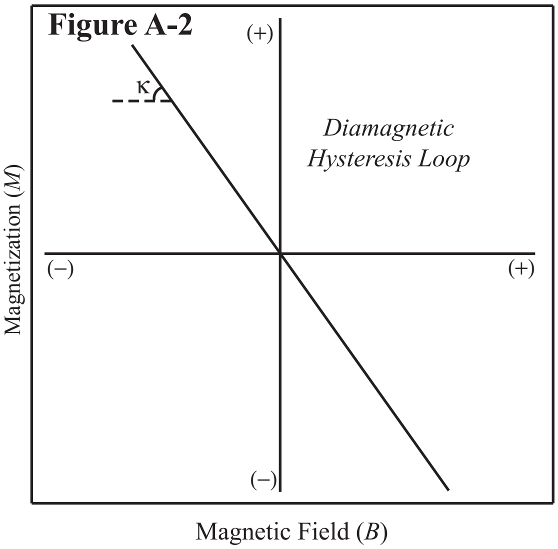
Figure A-2

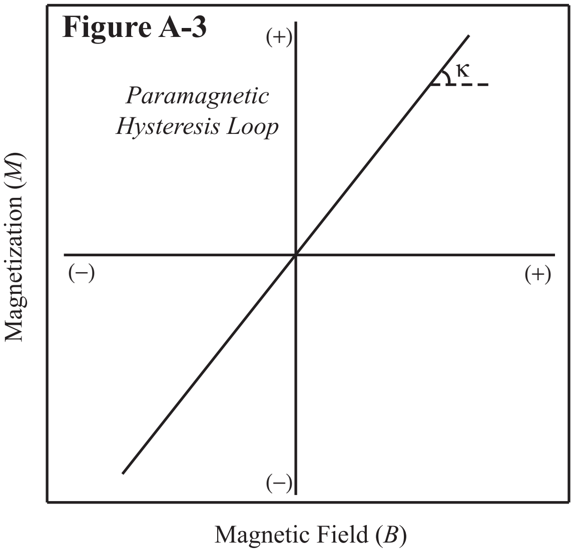
Figure A-3

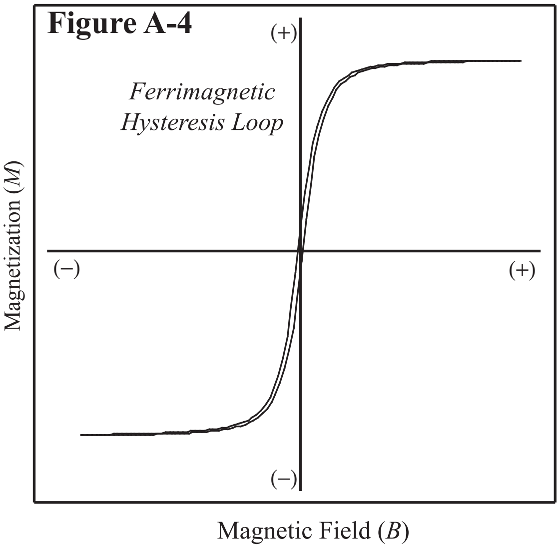
Figure A-4

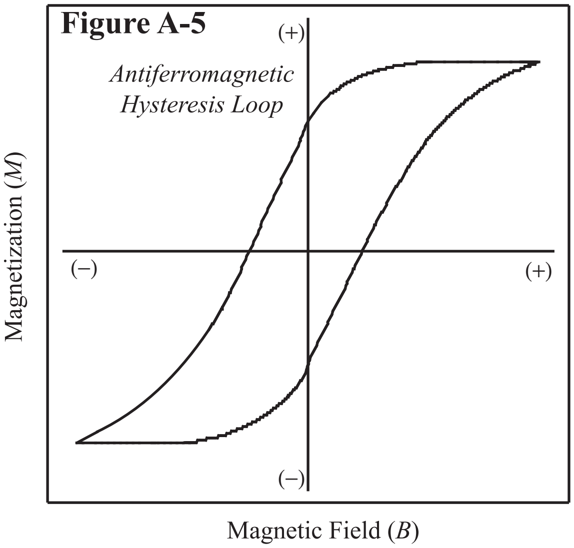
Figure A-5

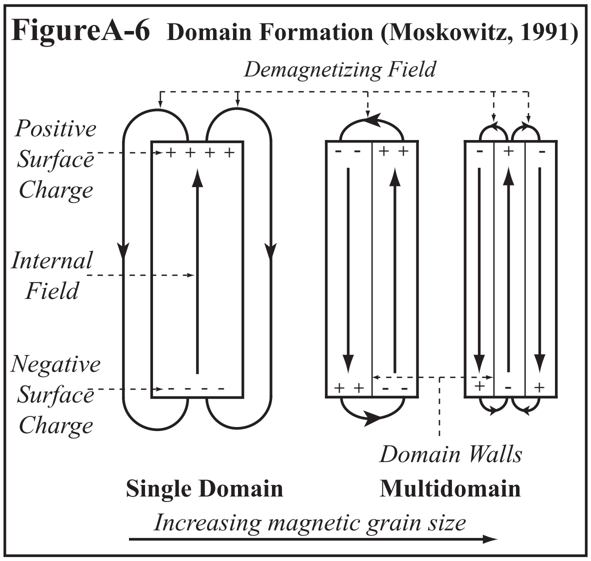
FigureA-6 **Domain Formation (Moskowitz, 1991)**

Figure A-7

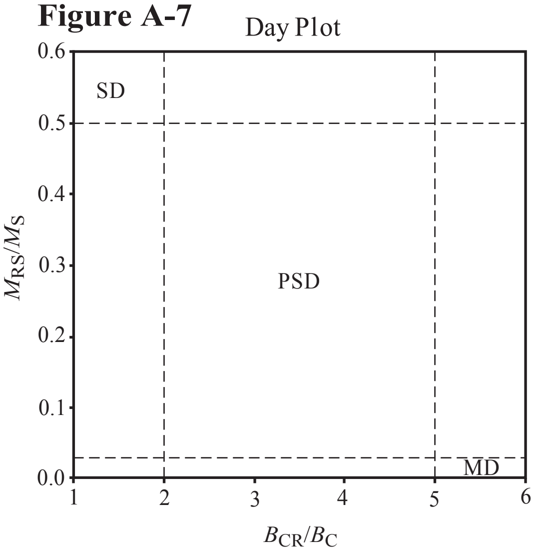

Figure A-8

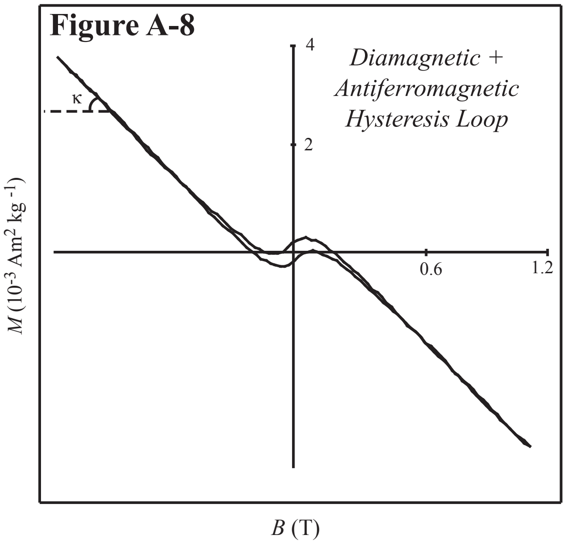

Figure A-9

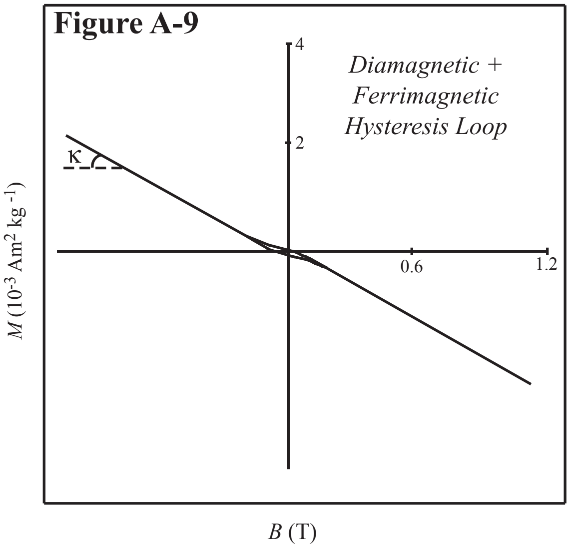

Figure A-10

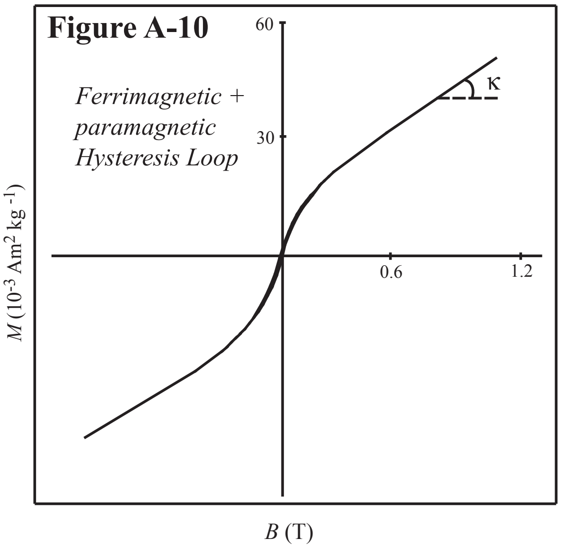

Figure A-11

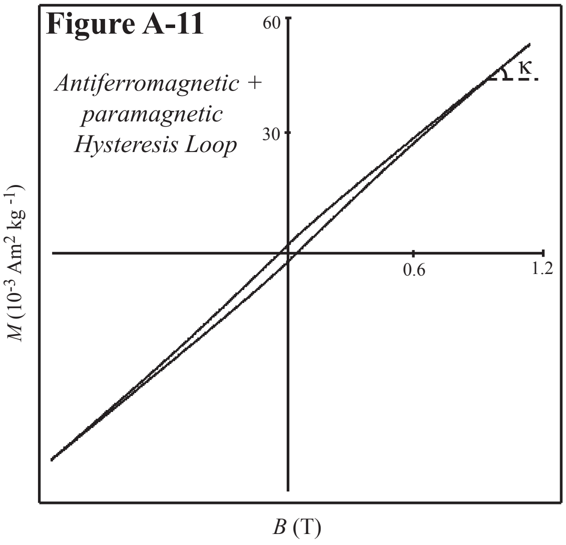

Figure A-12

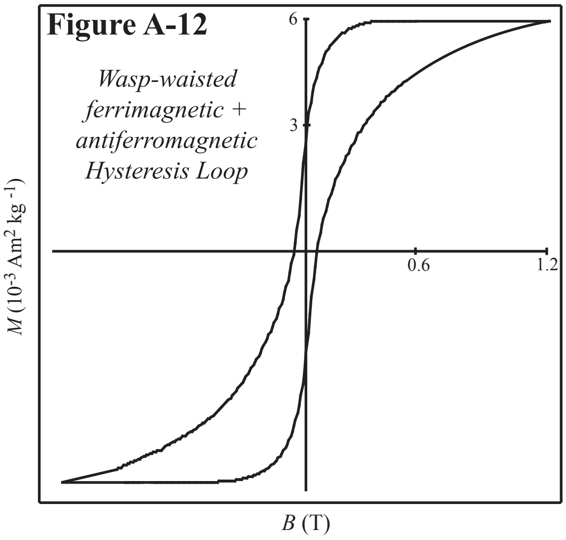

Appendix A - Figure Captions

Figure A-1 - Magnetic hysteresis loop showing the key parameters explained in the text. κ is the initial susceptibility given by the slope of the M-B curve at low fields.

Figure A-2 - Example of a diamagnetic hysteresis loop. The direction of magnetization in diamagnetic materials opposes the direction of the applied field leading to negatively sloped hysteresis loops. Since diamagnetic materials cannot acquire remanence, their loops trace out and intersect the origin when the field transitions from positive to negative, and vice versa. κ is the diamagnetic susceptibility given by the slope of the M-B curve at high fields and is used to calculate χ_d (the diamagnetic contribution to χ_{lf}).

Figure A-3 - Example of a paramagnetic hysteresis loop. In paramagnetic materials, the direction of magnetization is parallel to the direction of the applied field such that the loops are slope positive. Like diamagnetic materials, paramagnetic materials cannot acquire remanence and their loops trace out and intersect the origin when the field transitions from positive to negative, and vice versa. κ is the high-field susceptibility given by the slope of the M-B curve at high fields and is used to calculate χ_h (the paramagnetic + antiferromagnetic contribution to χ_{lf}).

Figure A-4 - Example of a ferrimagnetic hysteresis loop. The shape of the loop is sigmoidal and saturates easily at laboratory fields (< 0.8 T). The saturation point (M_S; Fig. A-1) is the point in which no more magnetization can be acquired by the sample with increasing field. The reason why ferrimagnetic samples are flat-topped is because they can reach saturation at laboratory applied fields. Furthermore, ferrimagnetic material can acquire remanence as shown by the open loop.

Figure A-5 - Example of an antiferromagnetic hysteresis loop. Antiferromagnetic materials commonly saturate at field well above those attainable by standard laboratory equipment. Furthermore, due to their higher coercivities they are harder to demagnetize and produce wide open loops at low fields.

Figure A-6 - Illustrative model of domain formation within magnetic grains. Surface charges form on the ends of grains due to magnetization and are a second source of a magnetic field (the demagnetizing field). The energy associated with this surface charge distribution is the magnetostatic energy. The magnetostatic energy can be greatly diminished if the magnetization splits into two domains magnetized in opposite directions. As particle size increases, it is energetically more favorable if domains form and reduce the magnetostatic energy.

Figure A-7 - Day plot illustrating the domain fields for magnetite. SD is single domain, PSD is pseudo-single domain, and MD is multidomain. Field distinctions are modeled after Dunlop and Ozdemir (1997).

Figure A-8 - Example of a mixture of diamagnetic and antiferromagnetic grains. The diamagnetic contribution is indicated by the negative high field slope and the antiferromagnetic contribution is indicated by the wide open loop at fields up to ~ 0.5 T. κ is the diamagnetic susceptibility given by the slope of the *M-B* curve at high fields and is used to calculate χ_d (the diamagnetic contribution to χ_{lf}).

Figure A-9 - Example of a mixture of diamagnetic and ferrimagnetic grains. The ferrimangetic contribution is indicated by the open loop at low fields. In contrast to antiferromagnetic mixtures, ferrimagnetic mixtures produce loops that are more constricted at low fields and close at fields commonly < 0.4 T. κ is the diamagnetic susceptibility given by the slope of the *M-B* curve at high fields and is used to calculate χ_d (the diamagnetic contribution to χ_{lf}).

Figure A-10 - Example of a mixture of ferrimagnetic and paramagnetic grains. The loop is slope positive for paramagnetic grains, in contrast to slopes for diamagnetic minerals. The ferrimagnetic contribution is indicated by a constricted loop at low fields. κ is the high-field susceptibility given by the slope of the *M-B* curve at high fields and is used to calculate χ_h (in this case the paramagnetic contribution to χ_{lf}).

Figure A-11 - Example of a mixture of antiferromagnetic and paramagnetic grains. The loop is slope positive for paramagnetic grains and is open at fields above 0.4 T, indicative of antiferromagnetic minerals. κ is the high-field susceptibility given by the slope of the *M-B* curve at high fields and is used to calculate χ_h (the paramagnetic + antiferromangetic contribution to χ_{lf}).

Figure A-12 - Example of a mixture of minerals with different coercivities (e.g. magnetite and hematite) that produce constricted hysteresis loops that are narrower in the middle and wider above and below. These types of loops are called “wasp-waisted” (Roberts et al., 1995).

References

Begét, J. E., D. B. Stone, and D. B. Hawkins, 1990, Paleoclimatic forcing of magnetic susceptibility variations in Alaskan loess during the late Quaternary: Geology, v. 18, p. 40-43.

Dearing, J., 1999, Magnetic Susceptibility, *in* J. Walden, F. Oldfield, and J. P. Smith, eds., Environmental Magnetism: a practical guide: Technical Guide No. 6, Quaternary Research Association, London, p. 250.

Dunlop, D. J., 2002, Theory and application of the Day plot (Mrs/Ms vs. Hcr/Hc) 2. Application to data for rocks, sediments and soils: Journal of Geophysical Research, v. 107, p. EPM 5-1 to 5-15.

Dunlop, D. J., and O. Ozdemir, 1997, Rock Magnetism: Cambridge, UK, Cambridge University Press, 573 p.

Evans, M. E., and F. Heller, 2003, Environmental Magnetism: Principles and Applications of Enviromagnetics: International Geophysics Series, v. 86, Academic Press, 299 p.

Henry, B., D. Jordanova, N. Jordanova, and M. Le Goff, 2005, Transformations of magnetic mineralogy in rocks revealed by difference of hysteresis loops measured after stepwise heating: theory and case studies: Geophysical Journal International, v. 162, p. 64-78.

Hrouda, F., P. Muller, and J. Hanak, 2003, Repeated progressive heating in susceptibility vs. temperature investigation: a new paleotemperature indicator?: Physics and Chemistry of the Earth, v. 28, p. 653-657.

Kelso, P. R., B. Tikoff, M. Jackson, and W. Sun, 2002, A new method for the separation of paramagnetic and ferromagnetic susceptibility anisotropy using low field and high field methods: Geophysical Journal International, v. 151, p. 345–359.

Moskowitz, B. M., 1991, Hitchhiker's Guide to Magnetism, Environmental Magnetism Workshop, pp. 1–38, Minneapolis, The Institute for Rock Magnetism and the Global Paleorecords Research Training Group.

Roberts, A., Y. Cui, and K. L. Verosub, 1995, Wasp-waisted hysteresis loops: Mineral magnetic characteristics and discrimination of components in mixed magnetic systems: Journal of Geophysical Research, v. 100, p. 17909-17923.

Smith, J. P., 1999, An introduction to the magnetic properties of natural materials, *in* J. Walden, F. Oldfield, and J. P. Smith, eds., Environmental Magnetism: a practical guide: Technical Guide No. 6, Quaternary Reasearch Association, London, p. 250.

Tarling, D. H., and F. Hrouda, 1993, The magnetic anisotropy of rocks: Chapman & Hall, London, 217 p.

Thompson, R., and F. Oldfield, 1986, Environmental Magnetism: Allen & Unwin, London, 227 p.